ELSEVIER

NeuroImage

www.elsevier.com/locate/ynimg
NeuroImage 28 (2005) 682 – 690

Diffusion tensor imaging in medial temporal lobe epilepsy with hippocampal sclerosis

Lionel Thivard,[a,b,*] Stéphane Lehéricy,[c,d] Alexandre Krainik,[e] Claude Adam,[a,f] Didier Dormont,[c,f] Jacques Chiras,[c] Michel Baulac,[a,b] and Sophie Dupont[a,b]

[a]*Epileptology Unit, Hôpital de la Salpêtrière, 75013 Paris, France*
[b]*INSERM U739, Faculté de Médecine Pitié-Salpêtrière, 105, Boulevard de l'Hôpital, 75013 Paris, France*
[c]*Department of Neuroradiology, Hôpital de la Salpêtrière, 75013 Paris, France*
[d]*Center for Magnetic Resonance Research, University of Minnesota School, Minneapolis, MN 55455, USA*
[e]*MRI Unit and Mixt Unit INSERM/Université Joseph Fourier U594, BP 217- CHU Grenoble, 38043 Grenoble cedex, France*
[f]*CNRS UPR640 LENA, Hôpital de la Pitié-Salpêtrière, 75013 Paris, France*

Received 14 March 2005; revised 6 June 2005; accepted 10 June 2005
Available online 9 August 2005

Interictal diffusion imaging studies in patients with medial temporal lobe epilepsy (MTLE) accompanied by hippocampal sclerosis (HS) have shown an increased diffusivity in the epileptogenic hippocampus. In this study, we wanted to explore the whole brain in order to determine if MTLE could have an impact on the organization and the architecture of a large cerebral network and to identify clinical factors that could mediate diffusion abnormalities. Diffusion tensor imaging (DTI) and statistical parametric mapping of the entire brain were performed in 35 well-defined MTLE patients and in 36 healthy volunteers. SPM analyses identified three abnormal areas: an increased diffusivity was detected in the epileptic hippocampus and the ipsilateral temporal structures associated with a decreased anisotropy along the temporal lobe, a decreased diffusivity was found in the contralateral non-sclerotic hippocampus, the amygdala, and the temporal pole, and finally, a decreased anisotropy was noted ipsilaterally in posterior extratemporal regions. Duration of epilepsy, age at onset, and the frequency of generalized tonic–clonic seizures or partial complex seizures did not correlate with the presence of diffusion abnormalities. Region of interest analysis in the hippocampus/parahippocampus demonstrated a correlation between lower ipsilateral diffusivity values and occurrence of epigastric aura and between higher anisotropy values in both hemispheres and history of febrile seizures. In conclusion, this study showed that diffusion abnormalities are not restricted to the pathologic hippocampus and involve a larger network. This pattern may indirectly reflect the epileptogenic network and may be interpreted as a cause or a consequence of epilepsy.

Keywords: Diffusion tensor imaging; Hippocampal sclerosis; Medial temporal lobe epilepsy

Introduction

Diffusion tensor imaging (DTI) is an imaging technique which permits visualization of the architecture of cerebral tissue. The magnitude (diffusivity) and the directionality (anisotropy) of molecular displacement by diffusion can be quantified using DTI (Pierpaoli et al., 1996). In epilepsy patients, a decreased diffusivity was first reported in cases of both focal (Wieshmann et al., 1997; Lansberg et al., 1999) and non-convulsive status epilepticus (Flacke et al., 2000; Chu et al., 2001). Decreased diffusivity has also been observed inconsistently in the early post-ictal period following focal short-lasting seizures (Diehl et al., 2001; Hufnagel et al., 2003).

In medial temporal lobe epilepsy (MTLE) patients with hippocampal sclerosis (HS), interictal diffusion imaging studies (Hugg et al., 1999; Wieshmann et al., 1999; Kantarci et al., 2002; Assaf et al., 2003; Londono et al., 2003; Lee et al., 2004; Duzel et al., 2004) found an increased diffusivity in the hippocampal region ipsilateral to the side of seizure focus. The majority of these studies have focused on the sole hippocampus using regions of interest (ROIs) methods. Anyway, there is a growing evidence from electroclinical data that in MTLE, the epileptogenic onset zone, i.e., the medial temporal lobe, is expanded to incorporate a larger epileptic network, i.e., larger cortical or subcortical regions involved in seizure propagation or in seizures control (Nair et al., 2004; Deransart et al., 2000; Chauvel, 2001). Numerous neuroimaging studies have demonstrated that structural or functional abnormalities (metabolic changes, subtle structural lesions) may extend beyond the seizure onset zone in unilateral MTLE associated with HS (Duncan, 1997; Bernasconi et al., 2003; Moran et al., 2001; Woermann et al., 1999; Tasch et al., 1999) even though the exact physiopathology of these abnormalities is still unknown.

In this study, DTI combined with statistical parametric mapping allowed us to explore the entire brain and to gain further insight

* Corresponding author. INSERM U739, Faculté de Médecine Pitié-Salpêtrière, 105, Boulevard de l'Hôpital, 75013 Paris, France. Fax: +33 1 42160300.
E-mail address: lionel.thivard@psl.ap-hop-paris.fr (L. Thivard).
Available online on ScienceDirect (www.sciencedirect.com).

1053-8119/$ - see front matter © 2005 Elsevier Inc. All rights reserved.
doi:10.1016/j.neuroimage.2005.06.045

into the organization and the structure of cerebral tissue in well-defined MTLE. This method provided a way to characterize diffusion abnormalities in a large network. To better determine clinical factors that might influence diffusion abnormalities to be associated with MTLE, we specifically studied the influence of epilepsy duration, age at onset, frequency of generalized tonic–clonic seizures (GTCS), frequency of complex partial seizures (CPS), or history of febrile seizures (FS).

Materials and methods

Patients and controls

The study population included 35 patients (24 women and 11 men, mean age 33.9 years ± 8.8, range 19 to 53 years) with MTLE who were undergoing presurgical evaluation for anterior temporal lobectomy at the epilepsy unit of the Salpêtrière hospital. The control group included 36 healthy volunteers (14 women and 22 men, mean age: 32.8 years ± 9.3, range 18 to 57 years) with no history of neurological disorders and normal standard MRI.

The proportion of women was larger in the group of patients than in controls (χ^2 test, $P = 0.012$). Four of the patients were left-handed, two of them exhibiting a left hippocampal sclerosis and the two others a right hippocampal sclerosis. All healthy volunteers but one reported to be right-handed. The remaining subject reported being left-handed in all daily living activities except writing.

Twenty-nine patients underwent a complete presurgical evaluation including medical, neurological, and neuropsychological examination, interictal EEG, and video-EEG monitoring. For the six other patients, video-EEG monitoring was planned. The diagnosis of unilateral HS was based on qualitative MRI assessment of hippocampal atrophy on T1-weighted images and high-signal on T2-weighted images. There were 18 left HS and 17 right HS. Patients with evident brain atrophy, ventricular enlargement, or visually bilateral abnormal hippocampus were not included in the study.

Clinical and MRI data including the side of the epileptogenic focus, the occurrence of febrile seizures, the age at onset and the mean duration of epilepsy, the existence and type of aura (abdominal, dysmnesic and/or emotional), and the frequency of CPS and of GTCS are reported in Table 1. We classed the frequency of GTCS as “rare” if a patient reported less than 10 seizures since disease onset and “frequent” when more than 10 seizures were reported.

The study was approved by the local ethics committee and informed written consent was obtained from all patients and healthy volunteers.

Imaging protocol

Conventional MRI and DTI data were acquired on a 1.5-T scanner (GE, Milwaukee, USA). Structural T1-weighted images (IR-FSPGR) were reviewed by experienced neuroradiologists to exclude potential abnormalities in control subjects. Patients reported to be free of seizure in the 24 h preceding the DTI scan.

Diffusion-weighted echoplanar images (EPI) were acquired with standard head coil for signal reception. Twenty axial slices were obtained using the following parameters: TR: 6500 ms, TE: 85 ms, flip angle 90°, acquisition matrix 128 × 128, reconstruction matrix 256 × 256, FOV 32 × 32 cm, in-plane resolution 1.25 × 1.25 mm, slice thickness of 5 mm with no gap. The acquisition was ungated.

Diffusion weighting was performed along 23 optimized non-collinear directions with two excitations resulting in 480 images acquired in less than 6 min. A single b value of 700 s/mm^2 was applied. In addition, a reference image with no diffusion weighting was also obtained (b_0 image).

Raw diffusion-weighted data were corrected for geometric distortion secondary to eddy currents using a registration technique based upon the geometric model of distortions (Haselgrove and Moore, 1996), as described by Lehericy et al. (2004).

Maps of fractional anisotropy (FA) and mean diffusivity (MD) which correspond to one third the trace of the diffusion tensor [Trace(D)/3] were calculated from the diffusion-weighted images.

SPM data analysis

To allow voxel-by-voxel statistical comparisons, the EPI images (T2-weighted images obtained for $b = 0$) of all subjects were spatially normalized to the standard EPI template provided in SPM99 using linear steps with 12 degrees of freedom and a 7 × 8 × 7 nonlinear warp. The origin for normalization was set manually to the anterior commissure. The diffusion maps were then normalized using the parameters determined from the normalization of the b_0 image. The normalized FA and MD maps were smoothed with a 10-mm isotropic Gaussian kernel. This filter size was chosen because we wanted to study the hippocampal area (for which a smaller filter size may be optimal) as well as other temporal and extratemporal structures (for which the dimension of the expected effects was probably larger than in the hippocampus). This relatively large filter size also allows the anisotropy data to conform more closely to a Gaussian field model by reducing the proportion of voxels exhibiting non-normally distributed residuals (Jones et al., 2005).

Statistical analysis was performed with all patients included as a single group. For this analysis, images were normalized such that all lesions were left-sided (e.g., images of patients with a right-sided HS were mirrored to the left side). The images of eighteen randomly-chosen controls subjects out of 36 were mirrored to match the patients group.

For all analysis, a statistical threshold of $P < 0.001$ was first applied (height threshold). An extent threshold of $P < 0.05$ corrected for multiple comparisons was then applied at the cluster level. For the hippocampal/parahippocampal region, small volume correction was also used with a mask drawn on the mean MD image of the patients using MRIcro software (310 voxels, $P < 0.05$ corrected for multiple comparisons within the volume of the hippocampal/parahippocampal region). A small volume correction was applied in this region because (i) the lesion was located in the hippocampal/parahippocampal region and (ii) the small size of this region could mask cluster significance when a correction based on the entire scanned brain volume was applied.

As brain structure, metabolism, and diffusion properties may change with age and differ between men and women (Pfefferbaum and Sullivan, 2003; Good et al., 2001; Van Laere et al., 2001), we tested the effect of age and sex on diffusion in patients and control groups. A positive correlation between MD and age was found in the two groups in several large cortical regions bilaterally, mainly in the frontal lobes. A negative correlation between FA and age was found bilaterally in the white matter underneath the frontal

Table 1
Clinical characteristics of the patients

Subjects	Age	Sex	Side	FS (age)	Age at onset (years)	Duration (years)	Frequency of GTCS	Number of CPS/month	Auras
1	42	W	L	Yes (8 months)	8	34	Frequent	4	d, e
2	21	W	R	No	1.5	19.5	Rare	3	a, e
3	37	W	L	Yes (1 year)	28	9	Rare	10	d
4	23	M	L	Yes (6 months)	13	10	Frequent	4	No
5	22	M	L	Yes (1 year)	1	21	Rare	8	a, d
6	33	M	L	Yes (2 years)	8	25	Frequent	4	d, e
7	27	W	R	Yes (1.5 years)	5	22	Rare	3	a
8	34	W	L	No	1	33	Rare	4	a
9	44	W	L	Yes (1.5 years)	6	38	Rare	4	e
10	32	M	L	No	3	29	Rare	8	a, e
11	23	W	R	Yes (4 months)	18	5	Rare	8	e
12	34	M	R	Yes (1 year)	12	22	Rare	10	a
13	52	M	L	Febrile coma (17 years)	24	28	Rare	2	e
14	35	M	L	Yes (6 months)	6	29	Rare	12	a
15	25	W	R	No	4	21	Rare	12	a
16	33	W	L	Yes (3 years)	13	20	Frequent	0	a
17	35	W	R	Yes (1 year)	27	8	Rare	3	a, d
18	25	W	R	Yes (6 months)	5	20	Rare	4	d
19	21	W	L	Yes (3 years)	14	7	Frequent	8	e
20	38	W	L	Yes (1.5 years)	7	31	Rare	2	a, d, e
21	29	W	L	No	13	16	Rare	10	a
22	34	W	R	Yes (2 years)	17	17	Rare	0	a
23	34	W	R	Meningitis (1 year)	31	3	Rare	0	a
24	39	W	L	No	6	33	Rare	2	a
25	28	W	L	Yes (1 year)	6	22	Rare	12	a
26	19	M	R	Yes (1.5 years)	12	7	Rare	16	d, e
27	34	M	R	No	30	4	Rare	8	a
28	38	W	R	No	17	21	Rare	4	a
29	50	W	R	No	28	22	Frequent	2	a, d
30	38	W	R	Yes (6 months)	14	24	Rare	4	a, d, e
31	43	M	R	No	4	39	Frequent	3	a, d
32	53	W	L	No	20	33	Rare	10	No
33	42	W	L	Yes (13 months)	17	25	Frequent	4	a
34	39	M	R	Yes	14	25	Rare	4	No
35	29	W	R	No	22	7	Frequent	1	a, d, e

W: woman; M: man; FS: febrile seizures; GTCS: generalized tonic–clonic seizures; CPS: complex partial seizures. Side refers to the side of the epileptogenic focus. a refers to abdominal, d to dysmnesic, and e to emotional aura.

lobes of both control and patients. No significant differences were found between male and female patients. In controls, an increased MD was found in men compared to women in the right temporo-parietal region and precentral gyrus.

We therefore used age and sex as confounding variables in further statistical analysis. Group comparisons using Ancova were performed between patients and control subjects, between patients with frequent (n = 9) and rare (n = 26) GTCS, between patients with (n = 21) and without (n = 14) febrile seizures, and between patients with or without each of the three types of aura. Multiple regressions were performed in patients for correlation of diffusion changes with age at onset, duration of epilepsy, and frequency of CPS.

Since we used the template provided by SPM99, brain region coordinates were obtained in the MNI space. We also present the coordinates and corresponding regions in the Talairach space (Talairach and Tournoux, 1988) derived with the algorithm given at http://www.mrc-cbu.cam.ac.uk/Imaging/Common/mnispace.

Finally, we investigated whether one of the underlying assumptions of SPM, i.e., the normality of the residuals, was met for anisotropy data. We followed the steps proposed by Jones et al. (Jones et al., 2005) and used the SPMd toolbox developed by Luo and Nichols to compute the Shapiro–Wilk (SW) statistic in each image voxel (Luo and Nichols, 2003). The number of voxels throughout the total brain volume with a P value < 0.05 was computed and expressed as a proportion of the total number of voxels analyzed (i.e., within the volume of the SPM mask). In a second step, we calculated whether there was any overlap in regions of significant patient–control differences (cluster corrected at P < 0.001) and regions in which residuals were deemed to be non-normally distributed.

ROI analysis

As a second step, we examined regions of interest in the hippocampal/parahippocampal region on both sides in all subjects. The values of the same eighteen randomly-chosen controls as for the SPM analysis were flipped to match the patients group. The aims of this analysis were (i) to demonstrate the magnitude of the effects obtained with SPM and (ii) to ask whether diffusion

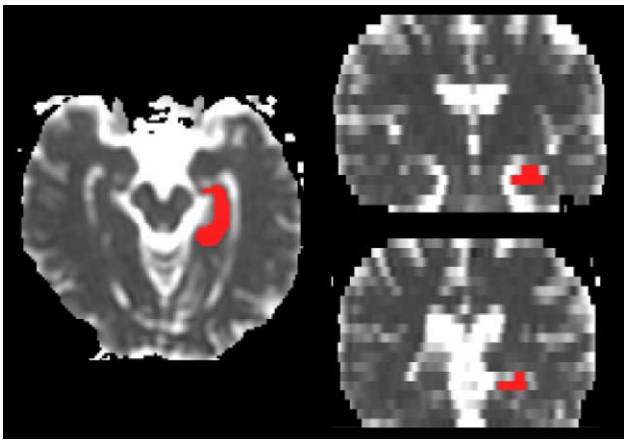

Fig. 1. Hippocampal/parahippocampal ROI in a control subject. The ROI is drawn on the native MD image and is displayed on one axial and two coronal slices.

abnormalities in this region were correlated with any clinical variables.

ROIs were drawn manually on the axial and coronal slices of the individual native diffusion images using MRIcro (Fig. 1). This software provided MD and FA values for each ROI.

Statistical analyses were conducted using statistical software (SPSS, version 11.5, Chicago, IL) in order to compare MD and FA values obtained on both sides in patients and controls, and to ask whether such values in patients were related to clinical characteristics (sex, age, age at onset, mean duration of epilepsy, history of FS, frequency of CPS and GTCS, and type of aura).

Results

Normality of residuals for anisotropy data

We found a proportion of 14.13% voxels with non-gaussian residuals, mainly in the cerebral peduncles and orbito-frontal region. The overlap between regions of significant patient–control differences (at $P < 0.001$ cluster corrected) and regions in which residuals were deemed to be non-normally distributed was 7.33%. We therefore assumed that it was an acceptable proportion of voxels with non-normally distributed residuals.

Group analysis between the whole group of patients and controls (Table 2 and Fig. 2)

Maps of mean diffusivity

Patients exhibited an increased MD in the temporal lobe ipsilateral to the epileptogenic focus. This increase was located along the hippocampal/parahippocampal region and also more laterally extending in the anteroposterior direction from the temporal pole to the temporo-occipital junction, partly in the white matter (Table 2 and Fig. 2).

A decreased MD was found in a cluster contralateral to the epileptogenic focus involving the amygdala and the temporal pole. Two clusters statistically significant using small volume correction were located on the same side in the anterior (30, −19, −22; Z score = 3.40; $P < 0.028$) and posterior parts (21, −35, −3; Z score = 3.77; $P < 0.017$) of the hippocampal/parahippocampal region.

Maps of anisotropy

A decreased FA was present in four brain regions, all located in the hemisphere ipsilateral to the epileptogenic focus. Two clusters were located in the white matter underlying the temporal lobe ipsilateral to the epileptogenic focus: one at the level of the temporal stem and the other more laterally extending from the temporal pole to the temporo-occipital junction. Another cluster was located in part along the arcuate fasciculus, involving frontal and parietal regions with an extension in the parieto-occipital junction. A smaller cluster was located in the cingulum and the corpus callosum.

No increased FA was found.

Correlation with clinical data

A regression analysis showed no significant correlation between the MD, FA and the age at onset, the duration of the epilepsy, or the frequency of CPS. There were no significant difference in MD or FA between patients with frequent GTCS and those with rare GTCS, and between patients with febrile seizures and those without. There were no significant differences in MD or FA between patients who exhibited different types of aura and those who did not.

Table 2
Brain regions exhibiting diffusion abnormalities in the group comparison between patients and controls

Brain area	Talairach coordinates (x, y, z)	T score	Cluster size (voxels)
Increased MD			
Hippocampal/ parahippocampal region	−30 −24 −21	7.05	240
WM underneath the temporal lobe	−45 −19 −22	5.20	
	−48 −27 −16	4.51	
	−42 −47 −10	4.28	
Decreased MD			
Amygdala	24 −4 −20	4.55	130
Temporal pole	33 5 −25	4.44	
	48 2 −23	4.24	
Anterior and posterior hippocampal/ parahippocampal region	30 −19 −22	3.40	3
	21 −35 −3	3.77	8
Decreased FA			
WM underneath the temporal lobe (stem)	−27 −9 −10	5.66	205
	−21 5 −10	4.04	
WM underneath the parietal lobe	−36 −37 27	5.28	209
WM underneath the frontal lobe	−30 −13 34	4.56	
WM underneath the parieto-occipital junction	−30 −57 19	3.71	
WM underneath the temporal lobe	−48 −38 −11	5.23	145
	−48 −27 −16	5.17	
	−39 −7 −27	4.50	
Cingulum	−15 −28 29	4.29	55
Corpus callosum	0 −16 20	3.48	

Coordinates are in Talairach space. Only the higher peaks per cluster are given, negative coordinates refer to the side ipsilateral to the epileptogenic focus. FA: fractional anisotropy; MD: mean diffusivity; WM: white matter.

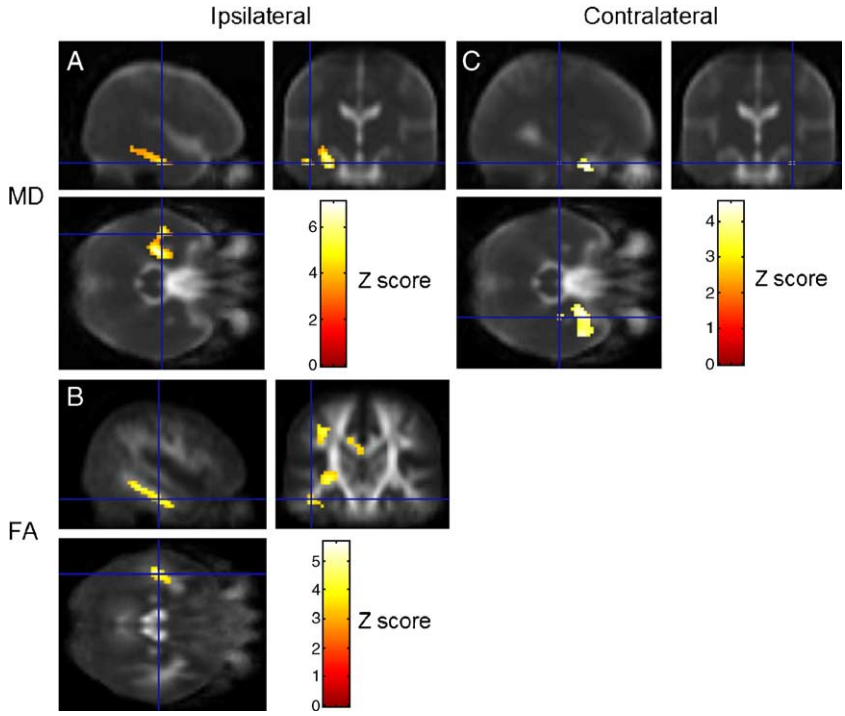

Fig. 2. Statistical parametric maps for the group comparison between patients and controls ($P < 0.05$ corrected for cluster extent). Images are superimposed on the patient's normalized average map. Left of the images corresponds to the side of the epileptogenic focus, right corresponds to the contalateral side. Brain regions showing (A) increased MD, (B) reduced FA, and (C) decreased MD in patients.

ROI analysis (Figs. 3 and 4)

In healthy volunteers, MD (mean ± SD, left: 926 ± 38 × 10^{-6} mm^2/s, right: 930 ± 41 × 10^{-6} mm^2/s) and FA values (left: 0.18 ± 0.02 and right: 0.19 ± 0.02) were symmetrical. In patients, MD values were smaller in the side contralateral to the epileptogenic focus (ipsilateral side: 960 ± 40 × 10^{-6} mm^2/s, contralateral side: 893 ± 26 × 10^{-6} mm^2/s) and FA values were symmetrical (ipsilateral side: 0.19 ± 0.02, controlateral: 0.19 ± 0.02) (Figs. 3 and 4).

An ANOVA was conducted with the MD value as the dependant variable, the within-subject factor being the measurement side (ipsi- or contralateral to the epileptogenic focus), and one inter-subject factor being the population group (patients or controls). The ANOVA revealed a significant interaction between the measurement side and the population group [$F(1,69) = 60.38$, $P < 0.001$], a significant main effect for the side of measurement [$F(1,69) = 92.89$, $P < 0.001$], and no main effect of the population group [$F(1,69) = 0,27$, ns]. Follow-up pairwise comparisons for side of measurement showed no difference in controls [t test(35) = 1.46, ns], whereas in patients, higher MD values were observed in the hippocampus ipsilateral to the epileptogenic focus [t test(34) = 11.25, $P < 0.001$]. Follow-up comparisons for population group showed higher MD values in the ipsilateral hippocampal/parahippocampal region than in controls [t test(69) = 3.10, $P = 0.003$], and lower MD values in the contralateral hippocampal/parahippocampal region than in controls [t test(69) = 3.80, $P < 0.001$]. Ipsi- and contralateral MD values were correlated in both groups (Pearson r coefficient = 0.50, $P = 0.003$ in patients, and $r = 0.73$, $P < 0.001$ in controls). In patients, inter-hemispheric differences in MD values were only correlated with ipsilateral MD values (Pearson r coefficient = 0.76, $P < 0.001$). Ipsilateral MD values were lower when patients had epigastric aura [t test(33) = 2.07, $P< 0.05$]. Contralateral MD values were not correlated to any clinical variable.

An ANOVA was conducted with the FA value as the dependant variable, the within-subject factor being the measurement side, and one inter-subject factor being the population group. No main effect or interaction was detected. Patients with history of febrile seizures

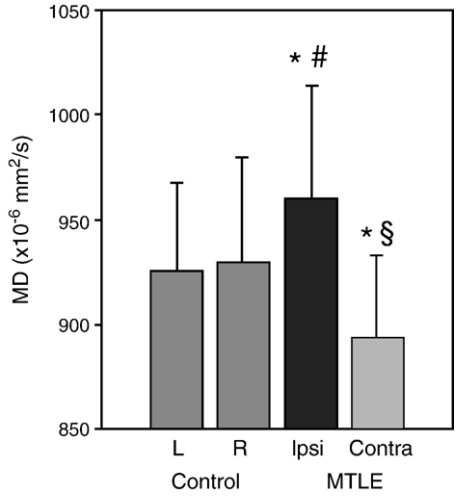

Fig. 3. Mean MD values and standard deviation for each side in patients and controls. In patients, higher MD values were observed in the hippocampal/parahippocampal region ipsilateral to the epileptogenic focus compared to the contralateral side (*$P < 0.001$). Patients exhibited higher MD values in the side ipsilateral to the epileptogenic focus compared to controls ($^{\#}P < 0.003$) and lower MD values in the side contralateral to the epileptogenic focus compared to controls ($^{\S}P < 0.001$).

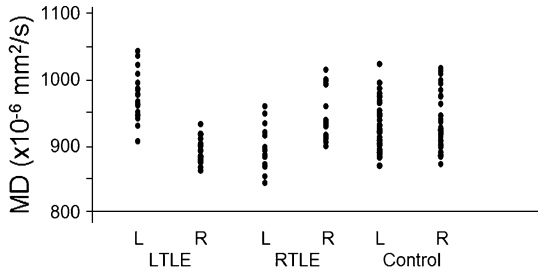

Fig. 4. Plot of individual MD values measured in the hippocampal/parahippocampal ROI for both sides in patients with left temporal lobe epilepsy (LTLE), right temporal lobe epilepsy (RTLE), and controls.

had higher FA values in both hemispheres [t test(33) = 2.35, P = 0.02 for ipsilateral hemisphere, and t test(33) = 2.38, P = 0.02 for contralateral hemisphere].

In all subjects, as MD values increased, FA values decreased (r = −0.26, P = 0.03 in ipsilateral hemisphere, and r = −0.34, P = 0.004 in contralateral hemisphere). These correlations were stronger in patients (r = −0.42, P = 0.013 in ipsilateral hemisphere, and r = −0.51, P = 0.002 in contralateral hemisphere).

Discussion

This study led to the findings that diffusion abnormalities are not restricted to the seizure onset zone, i.e., the pathologic hippocampus but extend in the adjacent temporal lobe, in the contralateral hippocampus, and in distant extratemporal structures. Furthermore, correlations were found between diffusion abnormalities and two of the clinical factors studied.

Diffusion abnormalities located into the epileptogenic zone

In MTLE associated with unilateral HS, the epileptogenic zone is not restricted to the sole sclerotic hippocampus and involves a larger regional network including the temporal pole and in some cases the temporal neocortex (Duncan, 1997). Interestingly, this work shows that diffusion abnormalities in MTLE patients also extended beyond the sclerotic hippocampus to lateral structures including the pole and the convexity. These results are in line with the notion of an epileptic zone exceeding the seizure onset zone and are complementary from previous studies that focused on the hippocampal region using ROI methods (Hugg et al., 1999; Wieshmann et al., 1999; Kantarci et al., 2002; Assaf et al., 2003; Londono et al., 2003; Duzel et al., 2004). Furthermore, increased MD in the temporal lobe beyond the hippocampal/parahippocampal region has also already been described by Lee et al. (2004). The existence of this increased diffusivity located in the epileptogenic zone does not seem to reflect different stages or severity of the epileptic syndrome since no correlation was found between diffusion abnormalities and the duration of epilepsy, the age at onset, the frequency of GTCS, or the frequency of CPS. Other hypotheses related to the seizure activity and/or the lesion itself, i.e., the hippocampal sclerosis, may be raised: neuronal loss, microstructural changes secondary to seizure propagation or deafferentation, partial volume effect. Hippocampal sclerosis is defined by a neuronal loss that selectively affects the CA1, 3, and 4 regions, resulting in atrophy that can be detected by MRI. Volumetric studies have also demonstrated atrophy in extrahippocampal medial temporal structures including the enthorinal and perirhinal cortices (Bernasconi et al., 2003). Neuronal loss in the temporal pole has been previously suggested by quantitative magnetic resonance imaging (Lencz et al., 1992), which revealed a decreased volume of the temporal lobes ipsilateral to the side of the seizure focus. Atrophy was also noted in the lateral regions of the temporal lobe corresponding to our area of increased MD (Moran et al., 2001). However, since previous diffusion studies found no correlation between the increased diffusivity and the degree of hippocampal atrophy (Wieshmann et al., 1999; Kantarci et al., 2002; Londono et al., 2003; Duzel et al., 2004), it seems unlikely that all the diffusion abnormalities may be explained by neuronal loss. This view is supported by the increased MD observed in medial temporal structures of MTLE patients with normal MRI (Rugg-Gunn et al., 2001).

Microstructural changes secondary to seizure propagation or to deafferentation are a second factor that might underlie diffusion abnormalities. Preliminary voxel-based morphometry studies have shown an excess of gray matter concentration (GMC) in the parahippocampal region of a large population of MTLE patients (Keller et al., 2002) that was attributed to a diminished gray–white matter demarcation and to underlying white matter abnormalities. Structural MRI studies have also demonstrated morphological abnormalities including the loss of gray–white matter differentiation in the temporal lobe of TLE patients (Mitchell et al., 1999). These changes did not result from dysplasia or inflammatory change, suggesting the possibility of myelin abnormalities affecting the temporal lobe ipsilateral to the seizure focus. Myelin-reduced density has finally been suggested by a volumetric MRI study (Coste et al., 2002) that demonstrated an increased T2-signal associated with reduced temporopolar white matter volume and by voxel-based morphometry that revealed a significant reduction of the temporal lobe white matter in unilateral TLE (Bernasconi et al., 2004; McMillan et al., 2004).

In our study, the increased MD was associated with a reduced FA along the white matter of the temporal lobe, which has not yet been described in MTLE patients with HS. The regions of reduced anisotropy that we observed included several major connection bundles of the temporal lobe, which are being described by fiber tracking (Catani et al., 2003; Powell et al., 2004). However, whether the abnormalities we described correspond to a cause (such as a developmental malformation possibly underlying the epileptogenic process) or a consequence (such as a structural modification induced by seizures) of MTLE and HS is still debated.

We found no modification in FA for the hippocampal/parahippocampal region. Previous studies using ROI have found lower anisotropy values than ours and have described a decreased anisotropy in the sclerotic hippocampus (Wieshmann et al., 1999; Assaf et al., 2003). These discrepancies across studies probably reflect great variations in methodology and in the amount of each anatomical region included in the ROIs.

Finally, a partial volume effect cannot be eliminated since atrophic processes may affect the entire hemisphere ipsilateral to the hippocampal sclerosis. However, previous studies using region of interest analysis to control for partial volume effect and hippocampal size have also shown increased diffusivity into the atrophic hippocampus (Hugg et al., 1999; Wieshmann et al., 1999; Kantarci et al., 2002; Londono et al., 2003).

Diffusion abnormalities located into the contralateral hippocampus

One of the most original findings of this study is the existence of a decreased MD in the contralateral medial temporal lobe. The peaks of the clusters were located in the amygdala, temporal pole, and anterior and posterior hippocampal/parahippocampal regions. No significant correlation was found in the contralateral hippocampus between these changes in MD and any of the clinical factors we studied.

Previous works, with smaller numbers of subjects, have reported variable MD values in the contralateral hippocampus of TLE patients. The contralateral hippocampal MD values were either normal (Hugg et al., 1999; Lee et al., 2004; Wieshmann et al., 1999; Kantarci et al., 2002; Duzel et al., 2004), or reduced without statistical significance (Assaf et al., 2003) or reduced in both the atrophic and normal hippocampi (Londono et al., 2003).

Methodological considerations might explain these discrepancies. These studies used different types of ROI which were often placed on a single slice and included a various amount of the hippocampal region. In contrast, we explored global diffusion abnormalities with whole brain SPM analysis without "a priori" hypothesis. To verify our first results in the hippocampal/parahippocampal region, we then conducted an ROI study on contiguous axial and coronal slices. Both methodologies brought the same results. Furthermore, the epileptic population used in our study was larger than previous studies, very homogeneous and carefully selected.

The finding of a contralateral MD decrease suggests a bilateral hippocampal involvement in MTLE. This result is in line with previous electroclinical, neuroradiological, and pathological evidences, which provide support for bilateral consequences of the MTLE syndrome (Spencer, 1998). Electroclinical studies have already demonstrated that seizures originating from the sclerotic hippocampus often spread to the contralateral non-sclerotic hippocampus. Many imaging studies also suggest that the contralateral temporal lobe is affected interictally in MTLE. Proton magnetic resonance spectroscopy has revealed bilateral abnormalities in 20% of MTLE patients (Woermann et al., 1999) that was sometimes correlated with the duration of epilepsy and the frequency of generalized tonic–clonic seizures (Tasch et al., 1999). Some authors (Cendes et al., 1997) postulated that controlateral reduction of NAA/Cr ratio could be related to the seizure activity that led to widespread functional changes of neurons and to reversible transsynaptic deafferentation of the contralateral temporal lobe. Others suggested that it might be related to a process of epiletogenesis generating independent contralateral interictal epileptiform discharges (Park et al., 2002). Whatever its primary pathophysiology, this impairment was related to a neuronal dysfunction rather that to a neuronal loss since spectroscopic abnormalities tended to normalize in the period after surgery (Cendes et al., 1997; Hugg et al., 1996; Vermathen et al., 2002).

Lastly, a recent work by Hogan et al. using MRI-based high-dimensional mapping has demonstrated a deformation of the contralateral hippocampal body different from that of the sclerotic hippocampus (Hogan et al., 2004). In agreement with this study, our results show that ipsilateral and contralateral hippocampal diffusion abnormalities are different, suggesting a distinct pathophysiology. Further studies are required to examine this interesting issue.

Diffusion abnormalities may help to gain further insight into the contralateral temporal abnormalities' pathophysiology. In epilepsy patients, a decreased MD was first described in the ictal or post-ictal period of focal or non-convulsive status epilepticus (Wieshmann et al., 1997; Lansberg et al., 1999; Flacke et al., 2000; Chu et al., 2001) and later, in some patients, during the post-ictal period after short MTLE seizures (Diehl et al., 2001; Hufnagel et al., 2003). Works on animal models of epilepsy also suggest that MD decreases after a seizure. Diffusion was reported to be depressed both during the period immediately following seizures induced by electroshock (Zhong et al., 1997) and at 24 h after status epilepticus induced by kaïnate injection in rats (Wang et al., 1996). We did not make EEG recordings systematically before or during the MRI session, and so cannot exclude the occurrence of subclinical seizures just before or during the examination. However, such subclinical activity seems unlikely for two reasons: (i) the ipsilateral hippocampal MD was significantly increased, (ii) the distribution of contralateral hippocampal MD values was homogeneous in our patients. Another hypothesis for the decreased MD is the existence of cytotoxic edema which may result from chronic ion channel dysfunction leading to cell swelling and extracellular space reduction (Binder et al., 2004). Although there is no direct evidence of this hypothesis in our data, experimental models have suggested that this phenomenon is present in epileptic areas but this remains very hypothetic. One mechanism could be the implication of the glial water channel aquaporin-4 (AQP4) which plays a role in the modulation of cerebral water balance and neural signal transduction and has recently been involved in seizure susceptibility in mice (Binder et al., 2004).

Extratemporal abnormalities

The major extratemporal diffusion abnormalities detected in this study consisted in a diminished FA both in part of the ipsilateral arcuate fasciculus involving frontal and posterior parietal regions as well as in the corpus callosum and cingulum.

The widespread brain abnormalities that we report are not a new finding in MTLE patients. FDG-PET studies have described extratemporal brain abnormalities, mostly in regions anatomically connected with the epileptogenic sclerotic hippocampus (Jokeit et al., 1997; Henry, 1996; Khan et al., 1997). To this regard, recent work showed that the anterior parahippocampal gyrus projects to the posterior temporal lobe and the extrastriate occipital lobe in healthy subjects (Powell et al., 2004). One previous study, using an ROI superimposed on a single slice in TLE patients, has shown a decreased FA in the posterior corpus callosum (Arfanakis et al., 2002), suggesting a more posterior involvement. Bilateral diffusion abnormalities were also recently demonstrated in the fornix and the cingulum of unilateral MTLE using fiber tracking (Concha et al., 2005). A work investigating gray and white matter volume with voxel-based morphometry reported a significant gray matter decrease in frontal, cingulate, and thalamic regions and a white matter reduction in parietal regions and in corpus callosum (Bernasconi et al., 2004). White matter reduction was also recently demonstrated with volumetric MRI in the frontal and parietal regions bilaterally and in the occipital lobe ipsilaterally (Seidenberg et al., 2005). The authors interpreted these abnormalities as a compromised connectivity of the epileptic temporal lobe with both cerebral hemispheres. Conversely to these studies, we did not find bilateral diffusion abnormalities in the fornix and the thalamus.

These discrepancies in the findings across studies are probably due to major technical and methodological differences.

Correlations with clinical data

Using the ROIs methodology, we found two significant correlations between clinical factors and diffusion abnormalities. The first correlation was between the ipsilateral MD within the sclerotic hippocampus and the existence of an epigastric aura. In those patients who exhibited an epigastric aura, the ipislateral hippocampal MD was lower.

Secondly, patients with history of febrile seizures had higher FA values in both hemispheres. This may be discussed either as the consequence of an initial precipitating event affecting the whole brain, i.e., febrile convulsions, or as the witness of a genetic background facilitating the occurrence of febrile convulsions and subsequent epilepsy.

In conclusion, diffusion abnormalities extending beyond the epileptogenic zone were observed in both hemispheres, revealing that MTLE has effects widely distributed throughout the brain. These diffusion abnormalities were different between the sclerotic and the contralateral hippocampus, apparently normal on MR images, suggesting that the underlying disease process in the contralateral hippocampus is different from HS. DTI is a recent neuroimaging technique and the morphological and functional implications of diffusion abnormalities remain to be fully understood. As the spatial resolution of DTI improves, it will provide even more detailed information on the pathophysiology of temporal lobe epilepsy, microstructure, and connectivity of the hippocampal region.

Acknowledgments

We wish to thank the physicians and the technical staff of the department of neuroradiology for their collaboration and assistance. We are grateful to Richard Miles for comments on the manuscript. This work was supported by the IFR 49 and by a grant from the Collège des Enseignants de Neurologie.

Appendix A. Supplementary data

Supplementary data associated with this article can be found, in the online version, at doi:10.1016/j.neuroimage.2005.06.045.

References

Arfanakis, K., Hermann, B.P., Rogers, B.P., Carew, J.D., Seidenberg, M., Meyerand, M.E., 2002. Diffusion tensor MRI in temporal lobe epilepsy. Magn. Reson. Imaging 20, 511–519.

Assaf, B.A., Mohamed, F.B., Abou-Khaled, K.J., Williams, J.M., Yazeji, M.S., Haselgrove, J., Faro, S.H., 2003. Diffusion tensor imaging of the hippocampal formation in temporal lobe epilepsy. Am. J. Neuroradiol. 24, 1857–1862.

Bernasconi, N., Bernasconi, A., Caramanos, Z., Antel, S.B., Andermann, F., Arnold, D.L., 2003. Mesial temporal damage in temporal lobe epilepsy: a volumetric MRI study of the hippocampus, amygdala and parahippocampal region. Brain 126, 462–469.

Bernasconi, N., Duchesne, S., Janke, A., Lerch, J., Collins, D.L., Bernasconi, A., 2004. Whole-brain voxel-based statistical analysis of gray matter and white matter in temporal lobe epilepsy. NeuroImage 23, 717–723.

Binder, D.K., Oshio, K., Ma, T., Verkman, A.S., Manley, G.T., 2004. Increased seizure threshold in mice lacking aquaporin-4 water channels. NeuroReport 15, 259–262.

Catani, M., Jones, D.K., Donato, R., Ffytche, D.H., 2003. Occipito-temporal connections in the human brain. Brain 126, 2093–2107.

Cendes, F., Andermann, F., Dubeau, F., Matthews, P.M., Arnold, D.L., 1997. Normalization of neuronal metabolic dysfunction after surgery for temporal lobe epilepsy. Evidence from proton MR spectroscopic imaging. Neurology 49, 1525–1533.

Chauvel, P., 2001. Contributions of Jean Talairach and Jean Bancaud to epilepsy surgery. In: Luders, H.O. (Ed.), Epilepsy Surgery. Lippincott Williams & Wilkins, Philadelphia, pp. 35–41.

Chu, K., Kang, D.W., Kim, J.Y., Chang, K.H., Lee, S.K., 2001. Diffusion-weighted magnetic resonance imaging in nonconvulsive status epilepticus. Arch. Neurol. 58, 993–998.

Concha, L., Beaulieu, C., Gross, D.W., 2005. Bilateral limbic diffusion abnormalities in unilateral temporal lobe epilepsy. Ann. Neurol. 57, 188–196.

Coste, S., Ryvlin, P., Hermier, M., Ostrowsky, K., Adeleine, P., Froment, J.C., Mauguiere, F., 2002. Temporopolar changes in temporal lobe epilepsy: a quantitative MRI-based study. Neurology 59, 855–861.

Deransart, C., Riban, V., Le, B., Marescaux, C., Depaulis, A., 2000. Dopamine in the striatum modulates seizures in a genetic model of absence epilepsy in the rat. Neuroscience 100, 335–344.

Diehl, B., Najm, I., Ruggieri, P., Tkach, J., Mohamed, A., Morris, H., Wyllie, E., Fisher, E., Duda, J., Lieber, M., Bingaman, W., Luders, H.O., 2001. Postictal diffusion-weighted imaging for the localization of focal epileptic areas in temporal lobe epilepsy. Epilepsia 42, 21–28.

Duncan, J.S., 1997. Imaging and epilepsy. Brain 120, 339–377.

Duzel, E., Kaufmann, J., Guderian, S., Szentkuti, A., Schott, B., Bodammer, N., Hopf, M., Kanowski, M., Tempelmann, C., Heinze, H.J., 2004. Measures of hippocampal volumes, diffusion and 1H MRS metabolic abnormalities in temporal lobe epilepsy provide partially complementary information. Eur. J. Neurol. 11, 195–205.

Flacke, S., Wullner, U., Keller, E., Hamzei, F., Urbach, H., 2000. Reversible changes in echo planar perfusion- and diffusion-weighted MRI in status epilepticus. Neuroradiology 42, 92–95.

Good, C.D., Johnsrude, I.S., Ashburner, J., Henson, R.N., Friston, K.J., Frackowiak, R.S., 2001. A voxel-based morphometric study of ageing in 465 normal adult human brains. NeuroImage 14, 21–36.

Haselgrove, J.C., Moore, J.R., 1996. Correction for distortion of echo-planar images used to calculate the apparent diffusion coefficient. Magn. Reson. Med. 36, 960–964.

Henry, T.R., 1996. Functional neuroimaging with positron emission tomography. Epilepsia 37, 1141–1154.

Hogan, R.E., Wang, L., Bertrand, M.E., Willmore, L.J., Bucholz, R.D., Nassif, A.S., Csernansky, J.G., 2004. MRI-based high-dimensional hippocampal mapping in mesial temporal lobe epilepsy. Brain 127, 1731–1740.

Hufnagel, A., Weber, J., Marks, S., Ludwig, T., De Greiff, A., Leonhardt, G., Widmann, G., Stolke, D., Forsting, M., 2003. Brain diffusion after single seizures. Epilepsia 44, 54–63.

Hugg, J.W., Kuzniecky, R.I., Gilliam, F.G., Morawetz, R.B., Fraught, R.E., Hetherington, H.P., 1996. Normalization of contralateral metabolic function following temporal lobectomy demonstrated by 1H magnetic resonance spectroscopic imaging. Ann. Neurol. 40, 236–239.

Hugg, J.W., Butterworth, E.J., Kuzniecky, R.I., 1999. Diffusion mapping applied to mesial temporal lobe epilepsy: preliminary observations. Neurology 53, 173–176.

Jokeit, H., Seitz, R.J., Markowitsch, H.J., Neumann, N., Witte, O.W., Ebner, A., 1997. Prefrontal asymmetric interictal glucose hypometabolism and cognitive impairment in patients with temporal lobe epilepsy. Brain 120, 2283–2294.

Jones, D.K., Symms, M.R., Cercignani, M., Howard, R.J., 2005. The

effect of filter size on VBM analyses of DT-MRI data. NeuroImage 26, 546–554.
Kantarci, K., Shin, C., Britton, J.W., So, E.L., Cascino, G.D., Jack Jr., C.R., 2002. Comparative diagnostic utility of 1H MRS and DWI in evaluation of temporal lobe epilepsy. Neurology 58, 1745–1753.
Keller, S.S., Mackay, C.E., Barrick, T.R., Wieshmann, U.C., Howard, M.A., Roberts, N., 2002. Voxel-based morphometric comparison of hippocampal and extrahippocampal abnormalities in patients with left and right hippocampal atrophy. NeuroImage 16, 23–31.
Khan, N., Leenders, K.L., Hajek, M., Maguire, P., Missimer, J., Wieser, H.G., 1997. Thalamic glucose metabolism in temporal lobe epilepsy measured with 18F-FDG positron emission tomography (PET). Epilepsy Res. 28, 233–243.
Lansberg, M.G., O'Brien, M.W., Norbash, A.M., Moseley, M.E., Morrell, M., Albers, G.W., 1999. MRI abnormalities associated with partial status epilepticus. Neurology 52, 1021–1027.
Lee, J.H., Chung, C.K., Song, I.C., Chang, K.H., Kim, H.J., 2004. Limited utility of interictal apparent diffusion coefficient in the evaluation of hippocampal sclerosis. Acta Neurol. Scand. 110, 53–58.
Lehericy, S., Ducros, M., Krainik, A., Francois, C., Van de Moortele, P.F., Ugurbil, K., Kim, D.S., 2004. 3-D diffusion tensor axonal tracking shows distinct SMA and pre-SMA projections to the human striatum. Cereb. Cortex 14, 1302–1309.
Lencz, T., McCarthy, G., Bronen, R.A., Scott, T.M., Inserni, J.A., Sass, K.J., Novelly, R.A., Kim, J.H., Spencer, D.D., 1992. Quantitative magnetic resonance imaging in temporal lobe epilepsy: relationship to neuropathology and neuropsychological function. Ann. Neurol. 31, 629–637.
Londono, A., Castillo, M., Lee, Y.Z., Smith, J.K., 2003. Apparent diffusion coefficient measurements in the hippocampi in patients with temporal lobe seizures. Am. J. Neuroradiol. 24, 1582–1586.
Luo, W.-L., Nichols, T.E., 2003. Diagnosis and exploration of massively univariate neuroimaging models. NeuroImage 19, 1014–1032.
McMillan, A.B., Hermann, B.P., Johnson, S.C., Hansen, R.R., Seidenberg, M., Meyerand, M.E., 2004. Voxel-based morphometry of unilateral temporal lobe epilepsy reveals abnormalities in cerebral white matter. NeuroImage 23, 167–174.
Mitchell, L.A., Jackson, G.D., Kalnins, R.M., Saling, M.M., Fitt, G.J., Ashpole, R.D., Berkovic, S.F., 1999. Anterior temporal abnormality in temporal lobe epilepsy: a quantitative MRI and histopathologic study. Neurology 52, 327–336.
Moran, N.F., Lemieux, L., Kitchen, N.D., Fish, D.R., Shorvon, S.D., 2001. Extrahippocampal temporal lobe atrophy in temporal lobe epilepsy and mesial temporal sclerosis. Brain 124, 167–175.
Nair, D.R., Mohamed, A., Burgess, R., Luders, H., 2004. A critical review of the different conceptual hypotheses framing human focal epilepsy. Epileptic Disord. 6, 77–83.
Park, S.A., Kim, G.S., Lee, S.K., Lim, S.R., Heo, K., Park, S.C., Chang, J.W., Kim, D.I., Lee, B.I., 2002. Interictal epileptiform discharges relate to 1H-MRS-detected metabolic abnormalities in mesial temporal lobe epilepsy. Epilepsia 43, 1385–1389.
Pfefferbaum, A., Sullivan, E.V., 2003. Increased brain white matter diffusivity in normal adult aging: relationship to anisotropy and partial voluming. Magn. Reson. Med. 49, 953–961.
Pierpaoli, C., Jezzard, P., Basser, P.J., Barnett, A., Di Chiro, G., 1996. Diffusion tensor MR imaging of the human brain. Radiology 201, 637–648.
Powell, H.W., Guye, M., Parker, G.J., Symms, M.R., Boulby, P., Koepp, M.J., Barker, G.J., Duncan, J.S., 2004. Noninvasive in vivo demonstration of the connections of the human parahippocampal gyrus. NeuroImage 22, 740–747.
Rugg-Gunn, F.J., Eriksson, S.H., Symms, M.R., Barker, G.J., Duncan, J.S., 2001. Diffusion tensor imaging of cryptogenic and acquired partial epilepsies. Brain 124, 627–636.
Seidenberg, M., Kelly, K.G., Parrish, J., Geary, E., Dow, C., Rutecki, P., Hermann, B., 2005. Ipsilateral and contralateral MRI volumetric abnormalities in chronic unilateral temporal lobe epilepsy and their clinical correlates. Epilepsia 46, 420–430.
Spencer, S.S., 1998. Substrates of localization-related epilepsies: biologic implications of localizing findings in humans. Epilepsia 39, 114–123.
Talairach, J., Tournoux, P., 1988. Co-Planar Stereotaxic Atlas of the Human Brain. Thieme, New York.
Tasch, E., Cendes, F., Li, L.M., Dubeau, F., Andermann, F., Arnold, D.L., 1999. Neuroimaging evidence of progressive neuronal loss and dysfunction in temporal lobe epilepsy. Ann. Neurol. 45, 568–576.
Van Laere, K., Versijpt, J., Audenaert, K., Koole, M., Goethals, I., Achten, E., Dierckx, R., 2001. 99mTc-ECD brain perfusion SPET: variability, asymmetry and effects of age and gender in healthy adults. Eur. J. Nucl. Med. 28, 873–887.
Vermathen, P., Ende, G., Laxer, K.D., Walker, J.A., Knowlton, R.C., Barbaro, N.M., Matson, G.B., Weiner, M.W., 2002. Temporal lobectomy for epilepsy: recovery of the contralateral hippocampus measured by (1)H MRS. Neurology 59, 633–636.
Wang, Y., Majors, A., Najm, I., Xue, M., Comair, Y., Modic, M., Ng, T.C., 1996. Postictal alteration of sodium content and apparent diffusion coefficient in epileptic rat brain induced by kainic acid. Epilepsia 37, 1000–1006.
Wieshmann, U.C., Symms, M.R., Shorvon, S.D., 1997. Diffusion changes in status epilepticus. Lancet 350, 493–494.
Wieshmann, U.C., Clark, C.A., Symms, M.R., Barker, G.J., Birnie, K.D., Shorvon, S.D., 1999. Water diffusion in the human hippocampus in epilepsy. Magn. Reson. Imaging 17, 29–36.
Woermann, F.G., McLean, M.A., Bartlett, P.A., Parker, G.J., Barker, G.J., Duncan, J.S., 1999. Short echo time single-voxel 1H magnetic resonance spectroscopy in magnetic resonance imaging-negative temporal lobe epilepsy: different biochemical profile compared with hippocampal sclerosis. Ann. Neurol. 45, 369–376.
Zhong, J., Petroff, O.A., Pleban, L.A., Gore, J.C., Prichard, J.W., 1997. Reversible, reproducible reduction of brain water apparent diffusion coefficient by cortical electroshocks. Magn. Reson. Med. 37, 1–6.